Molecular BioSystems

Accepted Manuscript

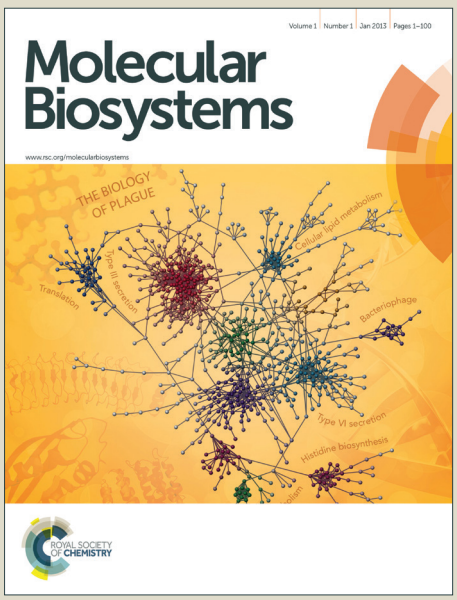

ROYAL SOCIETY OF CHEMISTRY

www.rsc.org/molecularbiosystems

Acclimatisation-induced stress influenced host metabolic and gut microbial composition change

Ivan K. S. Yap,[a*] Mee Teck Kho,[b] Swee Hua Erin Lim,[c] Nor Hadiani Ismail,[d] Wai Keat Yam,[a] Chun Wie Chong,[a]

[a] Life Sciences Department, School of Pharmacy, International Medical University, 126 Jalan Jalil Perkasa 19, Bukit Jalil, 57000 Kuala Lumpur, Malaysia

[b] School of Postgraduate Studies and Research, International Medical University, 126 Jalan Jalil Perkasa 19, Bukit Jalil, 57000 Kuala Lumpur, Malaysia

[c] Perdana University, Block B & D Aras 1, MAEPS Building, MARDI Complex, Jalan MAEPS Perdana, 43400 Serdang, Selangor DE, Malaysia

[d] Atta-ur-Rahman Institute for Natural Products Discovery, Universiti Teknologi MARA, 42300 Bandar Puncak Alam, Selangor DE, Malaysia

*To whom correspondence should be addressed: Ivan K. S. Yap, Life Sciences Department, School of Pharmacy, International Medical University, 126 Jalan 19/155B, Bukit Jalil, 57000 Kuala Lumpur, Malaysia. Tel., +60 3 2731 7474; E-mail, ivan_yap@imu.edu.my

Abbreviation: FID, free induction decay; NMR, nuclear magnetic resonance; TRFLP, terminal restriction fragment length polymorphism; TSP, sodium 3-(trimethylsilyl) propionate-2,2,3,3-d_4;

Running title: Metabolic and gut microbiotal changes in the mouse model during acclimatisation

Abstract

Understanding the basal gut bacterial community structure and the host metabolic composition is pivotal for the interpretation of laboratory treatments designed to answer questions pertinent to host-microbes interactions. In this study, we report for the first time the underlying gut microbiota and systemic metabolic composition in BALB/c mice during the acclimatisation period. Our results showed that stress levels were reduced in the first three days of the study when the animals were subjected to repetitive handling daily but the stress levels were increased when handling was carried out at lower frequencies (weekly). We also observed a strong influence of stress to the host metabolism and commensal compositional variability. In addition, temporal biological compartmental variations in the responses were observed. Based on these results, we suggest that consistency in frequency and duration of laboratory handling is crucial in murine models to minimise the impact of stress levels to the commensal and host metabolism dynamics. Furthermore, caution is advised in consideration of the temporal delay effect when integrating metagenomics and metabonomics data across different biological matrices (i.e. faeces and urine).

Introduction

Animal models form an essential part of biomedical research in the 21st century[1, 2] particularly with the advent of various omics platforms that generate large complex biological datasets.[3-5] Increasingly, multiple omics platforms in a single animal model were employed to generate comprehensive systems overview of a physiological state or disease pathophysiology.[6-9] Combination of metabonomic and metagenomic investigations have been used to shed light on the host-microbiome interactions and responses to metabolic diseases,[10] parasitic infections[7] and therapeutic interventions.[9, 11] Such a system biology approach has contributed greatly to the understanding of the link between host microbiome inhabiting the gut and host physiological conditions.[9-15]

The accuracy of host-microbe modelling is highly dependent on the complex microbiota composition and host basal metabolic phenotype prior to an intervention.[16-19] Factors contributing to the heterogeneity of the gut microbiome and metabolic profiles of experimental animals include various physiological factors such as diurnal variation, batch variation, age, gender, and species[5, 18, 20-22] as well as external environmental factors such as food and water intake, bedding and temperature. Amongst them, the latter has been closely correlated to the stress levels of the animals. Previous studies have shown that both invasive (e.g. bleeding, oragastric gavage etc) and non-invasive (e.g. cage changing cleaning and animal lifting etc) laboratory routines are likely to exert stress to the animals. The stressed animals usually exhibit abnormal physiological and immunological responses which compromised the reliability of the subsequent experimental observation.[23]

Thus, in order to normalise the basal physiological and gut microbial compositional difference in the experimental animals, standardisation in feed, incubation condition, and animal selection (e.g. weight, age, gender etc) is normally considered in the development of animal models. In addition, experimental animals usually undergo a period of acclimatisation before treatment to allow stabilisation of host physiology and gut ecosystem. Interestingly, however, the period of

acclimatisation is usually decided arbitrarily (Table 1). It is also still unclear whether both host metabolism and gut microbial dynamics respond at the same rate during acclimatisation.

Although various studies have been conducted to understand the effect of stress on animals, little attention has been placed on the stress levels exerted and its effect on the animals during acclimatisation prior to experimental treatments. Furthermore, current measures of stress were mainly focused on the behavioural or selected physiological responses of the animal such as the blood pressure, heart beat and corticosterone levels.[24-26] Only a few studies have examined the relationship between stress and overall metabolic profiles[5, 27] or gut microbiota status.[28, 29] In addition, an integrated systems biology approach utilising both metagenomics and metabolomics platforms have not been widely used to study the basal composition and stress responses of the gut microbiota and metabolic status of experimental animals.[30]

Here, we assess the basal metabolic and metagenomic variation and their responses in relation to stress during acclimatisation in the mouse-model for the first time using both nuclear magnetic resonance spectroscopy (NMR)-based metabonomics approach coupled with terminal restriction fragment length polymorphism (TRFLP) analyses. The data obtained from both platforms were statistically co-analysed to allow for systems level information recovery. Understanding the boundary of 'normality' within the host is paramount to ensure correct extraction of biological information from the experimental animals. Additionally, the pattern of change in experimental animals during acclimatisation will be essential to aid future experimental design in animal studies and delineating non-study specific biological variations.

Methods

Animals and sample collection

All animals used in this study were BALB/c female mice (5 weeks of age) purchased from the Institute for Medical Research (Kuala Lumpur, Malaysia). Animal experiments were carried out at the International Medical University (Kuala Lumpur, Malaysia), according to the guidelines and requirements of local and national authorities. Briefly, the animals were maintained at controlled environmental conditions (temperature: 26°C, relative humidity: 60-70%, light/dark cycle: 12/12 hours) with free access to water and standard rodent chow. In this study, urine and faecal samples were collected on day 1, day 2, day 3, day 8 and day 15. Faecal samples were collected for corticosterone assay and TRFLP analyses. Urine samples were collected for metabolic profiling. Faecal and urine sample collection took place between 0800 and 1100 hours to minimise diurnal variation in concentrations of biofluids.[18] At least 30 µL of urine and 6 faecal pellets were collected into Petri dishes without cross-contamination by gently rubbing the abdomens of the mice. Samples were transferred into 1.5 mL microcentrifuge tubes, immediately frozen and stored at −80 °C.

Corticosterone enzyme immunoassay from faecal material

Faecal corticorsterone measurement was used as a non-invasive technique to monitor stress levels in the laboratory animals. Corticosterone is a hormone secreted by the adrenal cortex when an animal is stressed and has been shown to be an accurate indicator of animal status.[31] This technique has been proven to be a reliable and accurate method for assessing physiological stress in experimental animals.[32, 33] Faecal material obtained from mice were measured for the levels of corticosterone using the Corticosterone Enzyme Immunoassay kit (Enzo Life Sciences, USA) with minor modifications to the sample preparation procedure. Prior to use, the faecal samples were dried overnight in an oven at 37 °C and powdered through mashing. The amount of starting material was weighed and 500 µL of Assay Buffer 15 from the kit was added to each sample. The samples were vortex-mixed for 15 s and left to stand for 5 min at room temperature. The samples were then centrifuged at 7000 rpm for 3 min. 100 µL of the supernatant was used for the assay according to manufacturer's instructions.

The level of corticosterone in each sample was calculated based on the standard curve obtained with reference to the weight used for each sample.

Urine sample preparation and ^{1}H NMR spectroscopic analysis

Urine samples were prepared by mixing 20 µL of urine with 30 µL of a phosphate buffer containing 90% D_2O and 0.25 mM 3-trimethylsilyl-1-[2,2,3,3-^{2}H4] propionate (TSP) and left to stand for 10 min. The resulting mixtures were then transferred into 5 mm NMR microbore tubes with 1.7 mm stem (Norell, USA).

A standard 1-dimensional (1-D) ^{1}H NMR spectrum was acquired for each sample with a pulse (recycle delay (RD)-90°-t_1-90°-t_m-90°-acquire free induction decay (FID)) on a Bruker AVIII 600 MHz spectrometer (Bruker Biospin, Fallenden, Switzerland) with a 5 mm BB(F)O broadband probe operating at 600.13 MHz (ambient probe temperature 27 °C). Samples were automatically delivered to the spectrometer by a Bruker SampleCase^{TM}. The field frequency was locked on D_2O solvent. The water peak was suppressed by gradient water presaturation during the RD of 4 s and mixing time (t_m), of 0.01 s. The 90° pulse length was adjusted to ~ 10 µs and an acquisition time of 2.65 s was used. In total, 32 transients were collected into 64 K data points using a spectral width of 20 ppm. An exponential line broadening function of 0.3 Hz was applied to the free induction decay prior to Fourier transformation.

Faecal DNA extraction and TRFLP analyses

DNA was extracted using QiAmp DNA stool mini kit (Qiagen, USA) according to the manufacturer protocol. The TRFLP was carried out as described in Chong *et al* [34] with minor modifications. Briefly, PCR was conducted using universal primers (27F and 1492R) targeting bacterial 16S rRNA gene region. Both primers were tagged with the fluorescence dye phosphoramidite fluorochrome 5-carboxyfluorescein (FAM) and 6-carboxy-hexachlorofluorescein (HEX) at 5' respectively. The

amplicons were digested using a 4-base cutter MSP-1 before subjected to electrophoretic separation using ABI 3100 and ABI 3730XL genetic analysers (Applied Biosystems, USA). ROX labeled GeneScan 500 control was used as size standard. The resulting fragment profiles were scored, aligned and noise filtered using the web-based programme T-REX.[35] Noise filtered procedure was carried out by removing peaks which are lower than the overall standard deviation. In addition, alignment was carried out by binning the peaks into TRFs with the clustering threshold of 0.5 bp, starting from the smallest peak among all the profiles. [36]

Data processing and analysis

For metabonomics analysis, ^{1}H NMR spectra of urine samples were manually phased and baseline-corrected using Bruker TopSpin (Version 3.1, Bruker Biospin, Fallenden, Switzerland). All spectra were referenced to the TSP resonance at δ 0.00. The complete spectra (δ 0.0-10.0) were digitised into 7K data points using an in-house developed MATLAB script (O. Cloarec, Imperial College London). The region containing the water resonance (δ 4.5-6.5) was removed from each spectrum to eliminate baseline effects of imperfect water suppression. In addition, the regions δ 0.0-0.5 and δ 9.2-10.0 containing only noise were removed. For each spectrum, normalisation to the total sum of the residual spectrum was carried out prior to pattern recognition analyses followed by scaling of the data to unit variance. Both unsupervised (principal component analysis, PCA) and supervised multivariate data analysis methods (projection to latent structures-discriminant analysis, PLS-DA and orthogonal partial least squares discriminant analysis, O-PLS-DA[37, 38]) were employed to visualise and interpret experimental differences. The statistical significance and validity of subsequent results were calculated using a permutation test (number of permutations = 1 000).[39] The covariance plot was used to aid interpretation of the significance of each metabolite from the permutation tests. The colours projected onto the spectrum indicate the significance of the metabolites with blue indicating no significance difference at $p > 0.05$ confidence levels and red indicating high significance difference at $p < 0.05$. In this study, only metabolites with $p < 0.01$ will be considered significant.

The TRFLP data obtained from T-REX was exported into PERMANOVA + add-on of the PRIMER6 multivariate data analysis package (Plymouth Marine Laboratory, UK) for analyses. Alpha-diversity indices including Shannon diversity index (*H'*) and Pielou's measure of species evenness (*J'*) were calculated using the DIVERSE option. For multivariate-analyses, the data was pre-treated with unit variance normalisation procedure before generating a Euclidean distance matrix which was used to perform permutational multivariate analysis of variance (PERMANOVA) and PCA. The PERMANOVA was carried out to test for gut microbial compositional difference between the groupings while the PCA was used to visualise the distribution of the samples across the sampling points. The significance of the PERMANOVA was calculated based on 999 permutations and corrected using Monte Carlo correction.

To test for the agreement between urine metabolite profiles and gut microbial composition, the two distance matrices were correlated using spearman rank correlation under 999 permutations. Two separate distance based linear modelling (DISTLM) were carried out to regress the urine metabolites on the bacterial assemblage pattern and with the opposite order (i.e. regress the T-RFLP peaks on the metabolites data cloud). The parsimonious model was constructed using stepwise selection under the second-order bias-corrected Akaike information criterion (AICc).[40] Specifically, the stepwise selection procedure allow both forward inclusion and backward elimination of the variables while the AICc was used to account for the large number of predictor variables (q) in relatively small number of samples (N).

Results

Faecal corticosterone measurements

Faecal corticosterone level of samples collected on 5 different days within a 15-day period showed a decreasing trend from day 1 to day 3 (decreasing from the highest level to the lowest level), after

which, the level of corticosterone increased from day 3 onwards to day 15 (Table 2). The level of corticosterone in samples collected from days 8 and 15 were not significantly different from the samples collected from days 1 and 2. The statistics indicated that the level of corticosterone was only significantly lower on day 3 as compared to day 1.

Effects of acclimatisation and the associated stress on 16S rRNA gene-based gut microbiota profiles

An opposite trend was observed for the bacterial diversity in the faecal samples. The lowest bacterial diversity was observed in the faecal samples collected on day 1 and day 2, while the highest bacterial diversity was found on day 3, corresponding to the lowest level of the stress biomarker (corticosterone). Subsequently, a reduction in diversity was detected from the samples collected on day 8, followed by a slight recovery in diversity on day 15.

PERMANOVA analysis of the TRFLP data suggested a significant difference in bacterial profiles at $P = 0.001$ (Pseudo-$F = 5.82$). A follow-up PCA was conducted to examine the distribution of the data. Fig. 1A showed a clear distinction between samples collected from day 3 as compared to those collected from other time points indicating that the day 3 samples showed the most distinct bacterial TRFLP profiles. It is interesting to note that the distinction is consistent with the sample having lowest mean corticosterone level among the total collected samples (Table 2). A PCA mean trajectory plot was drawn to detect the presence of finer separation within the sample cluster other than replicates from day 3 (Fig. 1B). From the trajectory plot, the biggest faecal bacteria compositional change occurred from day 2 to day 3 along the first principal component (PC1) followed by a movement along PC1 of almost the same magnitude to day 8 in the opposite direction before shifting along the second principal component (PC2) to day 15 indicating there was a clear time-dependent faecal bacteria development profile.

Effects of acclimatisation and the associated stress on urinary metabolic profiles

Median ^{1}H NMR spectra of urine obtained from all time points showed almost similar metabolic composition dominated by a number of metabolites such as short chain fatty acids (SCFA) i.e. 3-D-hydroxybutyrate and α-hydroxy *N*-valerate, tricarboxylic acid cycle intermediates i.e. pyruvate and citrate, methylamines i.e. trimethylamine and trimethalyamine *N*-oxide, creatine, creatinine, taurine, phenylacetylglycine and hippurate (Fig. S1). Visual inspection of the NMR spectra showed subtle differences in overall metabolic composition among the time points with the exception of urinary NMR spectra obtained on day 8, where relatively lower concentrations of urinary hippurate and citrate, and higher concentrations of urinary phenylacetylglycine and taurine were observed.

The urinary metabolic perturbations during acclimatisation were compared using PERMANOVA under Monte Carlo correction (999 permutations). Based on the results, the urine profiles were significantly different at P = 0.001 (Pseudo F = 4.46). The distribution of the data was further visualised using a principal component analysis based on the entire NMR data set. A total of 5 PCs were calculated for a PCA model using unit variance-scaled spectral data shown in Fig. 2A. In contrast to the gut microbiota profiles where sample with lowest stress level (day 3) showing apparent separation from other time points, a clear separation can be observed between urine samples obtained on day 8 as compared to all the other time points along PC1, whereas urine samples collected on day 1 were partially separated from the main cluster of samples along PC2. PCA trajectory analysis was used to give an overview of the metabolic alterations during acclimatisation (Fig. 2B). Three clear clusters can be observed in the urinary metabolic space, separating samples collected on day 1, day 8 and the remaining three time points (day 2, day 3 and day 15). The metabolic trajectory shifted from day 1 to day 2 along the PC2 followed by a slight shift along PC1 from day 2 to day 3. The biggest shift in metabolic trajectory occurred on day 8 along PC1 before returning to day 2 and day 3 metabolic spaces by day 15 along PC1.

In order to identify metabolites that are significantly different between each time point pairs, pair-wise O-PLS-DA models were constructed for each comparison of two time points based on two PLS and one orthogonal component with unit variance scaling. In addition, permutation testing was carried out on each pair-wise model to identify metabolites that are significantly different. The total explained variation for the NMR data was indicated by the R^2 value and the corresponding parameter indicating the predictive performance of the model (Q^2) reflected a high predictive ability (> 60% for all pairs except two (day 2 vs day 3 and day 2 vs day 15) Supplementary Table S1). All pair-wise models involving urine collected from mice on day 8 exhibited high Q^2 values, which is in agreement with the PCA scores plot (Fig. 2A) showing samples from day 8 clearly separated from the other time points. In these models, urine collected from mice on day 8 showed elevated 2,3-dihydroxybutyrate, α-hydroxy *N*-valerate, D-3-hydroxybutyrate, phenyalacetylglycine, succinate, taurine, trimethylamine, trimethylamine *N*-oxide, arginine and *N*-acetyls of glycoproteins, together with decreased levels of 2-oxoglutarate, acetate, citrate, dimethylglycine, formate, fumarate, guanidinoacetate, hippurate, *N*-methyl nicotinate, pyruvate and sarcosine (Supplementary Table S1).

In contrast, changes in urinary metabolites were less pronounced when urine NMR spectra collected from the remaining time points were compared against each other. Elevated urinary creatine, dimethylglycine, guanidinoacetate and phenylacetylglycine, and decreased urinary trimethylamine *N*-oxide were observed when comparing urine collected on day 1 against urine collected on day 2 and day 3 respectively (Supplementary Table S1). Urine collected on day 1 also showed relatively higher levels of 2-oxoglutarate, citrate and pyruvate, and lower levels of taurine, trimethylamine, trimethylamine *N*-oxide and tryptophan as compared to urine collected on day 15. Urine collected on day 2 and day 3 showed, by far, the least difference when compared with only one significantly different metabolite, 2-oxoglutarate. Similarly, when comparing urine collected on day 3 against urine collected on day 15, only one significantly different metabolite was identified, creatine. The results from O-PLS-DA and permutation tests on the latter were reflective of the scores and mean

trajectory plots (Fig. 2A and B), which showed no clear discrimination between these three time points.

Correlation and linear modelling of the urine metabolic profiles and gut microbiota

Due to the difference in the assemblage pattern, no significant correlation was found between the unit variance normalised Euclidean Distance matrices of both urine metabolites and gut microbial profiles (Spearman ρ = -0.04, P = 0.69). We further modelled the relationship separately using urine profiles as the predictor for gut microbiota distance matrix, followed by matching the distribution of the gut microbiota distribution using the urine metabolite profiles as predictor. According to the AIC selection criterion (with second order bias correction), 9 TRFLP peaks (Table 3A) were chosen to model the changes of the urine metabolite pattern over the 5 time points (cumulative R^2 =41.11%). We attempted to relate the putative identity of the TRFLP peaks by comparing to the TRF lengths generated via *in-silico* digestion, however the virtual digestion of the 16S rRNA gene database from ribosomal database project (>1200 bp) did not yield matchable identity (data not shown). Conversely, 6 ^{1}H-NMR peaks were selected using the same criterion to model the variation in gut microbial composition over the 15 days acclimatisation experiment (Table 3B). They included dimethylamine (2.77 ppm), fumarate (6.55 ppm), hippurate (3.99 ppm), α-hydroxy *N*-valerate (0.93 ppm), malonate (3.14 ppm, tentative assignment) and unknown 1 (6.99 ppm). Together, a combination of the 6 variables explained 29.1% of the total variance in the model.

Temporal effect of urine metabolites and gut microbiota composition

Despite the overall dissimilarity between the distribution pattern of PCAs generated using the urine (Fig. 1) and stool profiles (Fig. 2), a similar trend was observed between the urine metabolite profile obtained from days 2, 3, 8 and 15 with the gut microbiota composition derived from days 1, 2, 3 and 8. We speculated that such a pattern might be indicative of a delayed response in the urine metabolites in comparison to the gut microbial composition. To support our postulation, we

repeated the correlation analysis by matching the sample labelling of the urine and stool samples, accounting for one time point response delay in the urine metabolite profile (Fig. S2). The results showed a significant correlation at Spearman $\rho = 0.209$ ($P = 0.015$). However, DISTLM modelling using the relabelled data did not show a significant improvement in the overall predictive power. R^2 of 0.4187 was obtained when the urine profile was modelled using the relabelled gut microbial composition pattern. On the other hand, R^2 of 0.2761 was obtained when the relabelled gut microbial distribution was modelled using the urine metabolites composition. Nonetheless, the association of 2,3-dihydroxybutyrate (microbial associated metabolites, 1.223 ppm) to the gut microbial pattern was apparent in the relabelled data, accounting for nearly 14% of the overall variance in the model.

Discussion

By integrating both metagenomic and metabonomic approaches, we were able to show that the basal host metabolic and gut microbiological profiles were significantly affected during acclimatisation. The diversity and compositional changes of host gut microbe were shown to relate to host stress levels, potentially due to routine faecal and urine collection procedure; and that the gut microbe composition and host metabolic responses to the acclimatisation-induced stress may be operating on a different time scale. We postulated a potential delayed effect in the latter in comparison to the former. Overall, the stress level, gut microbiota composition and urine metabolite profiles were reasonably stable throughout the duration of the entire study (15 days).

Host responses to laboratory procedure -induced stress

All animals, including humans, undergo an adaptation process known as 'acclimatisation' when they are introduced or placed in a new environment.[41] Such a process takes time to normalise and usually invokes stress, which in turn induces metabolic changes in the hosts.[5] Indeed, studies have shown that experimental animals do habituate to frequencies of handling, which may introduce bias to host

sleep homeostasis and stress levels.[42, 43] As such, sufficient acclimatisation period should be factored into any animal study design to allow for stabilisation of host metabolic and gut microbe composition to enable useful extraction of biological information and inference. Our current study showed that the faecal corticosterone level was significantly reduced by day 3 of acclimatisation (Table 2), and subsequently increased by day 8 and day 15. This is further supported by our study sampling regime when sample collection was carried out on days 1, 2, 3, 8 and 15, with the highest frequency of handling in the first three days followed by a longer sampling time interval on days 8 and 15. The changes in corticosterone levels indicated that experimental animals do habituate to repeated handling as observed by the significantly lower levels of faecal corticosterone by day 3, and the subsequent increase in faecal corticosterone levels coincided with the longer sampling time interval on days 8 and 15. Our finding is in line with Leussis and Bolivar[41] who suggested that habituation is common among rodents and that the level of habituation is strongly related to the duration (i.e. intra session habituation) and frequency (i.e. inter session habituation) of handling. Initially, we speculated that the animals were habituated to the frequency of handling by the third day, but the memory to the handling routine dissipated over time as seen in the elevated corticosterone level in day 8 and day 15 samples. Thus, the interval between handling should be consistent in order to minimise fluctuations in the stress level across the study period.

Our study also showed that animal stress levels may have a direct influence on the host gut microbe diversity (Table 2) as well as composition (Fig. 1A). This was substantiated with the faecal samples collected on day 3 showing the highest bacterial diversity and significantly different gut microbe composition, both of which coincided with the lowest corticosterone levels. Studies pertinent to effect of stress on gut microbiota composition dates back to the 70s, when Tannock and Savage[44] showed that stressed mice harboured strikingly reduced lactobacilli in their gut. In addition, studies have shown that stress factors such as pups-mother separation, confinement (water avoidance stress) and social disruption affects the diversity of gut microbiota in experimental animal models. [28, 45, 46]

Our result provided additional support that the stress induced by non-invasive laboratory routines during acclimatisation can also impact on the gut bacterial composition.

Surprisingly however, the urinary metabolic changes on day 3 were unremarkable. Overall metabolite profiles of day 3 were similar to other samples (Fig. 2) except for a few metabolites that are known to be metabolised both by the host and the commensal flora (microbial-mammalian co-metabolites) such as hippurate that was elevated and trimethylamine *N*-oxide and 3-D-hydroxybutyrate which were reduced in comparison to the metabolite profiles of day 8 (Supplementary Table S1). It is interesting to note that from the urinary mean trajectory plot (Fig. 2B), although the metabolic composition changes over time, it returned to initially stable levels similar to that of day 2 and day 3 by day 15 as evidenced by the relatively lower number of metabolites perturbed (Supplementary Table S1). However, the opposite was observed in the faecal microbe composition where a progressive change in direction of the compositional trajectory occurred throughout the entire 5 time points indicating compositional changes occurs through time. This observation highlighted one of the commonly overlooked challenges when conducting metagenomics studies wherein the "stability" of the faecal microbe composition in experimental animals is difficult to attain even after fifteen days of study.

Temporal intercompartmental biological variation

In contrast to the corticosterone level as well as the gut microbe compositional variations when samples collected on day 3 showed most significant differences (Fig. 1 and Fig. 2), urine samples collected on day 8 showed the biggest metabolic variation as compared to other time points. The discrepancy could be explained by the presence of temporal inter-compartmental biological variation whereby the changes in gut microbe composition would not be reflected immediately in the urine samples on the same day. Indeed, a significant correlation was obtained when the gut microbiota composition was compared with the relabelled (to account for 1 time point delay) urine metabolite

profiles. Furthermore, the reduction in the rodent stress related marker such as hippurate[47] in urine of day 8 coincided with the lower stress and elevated bacteria diversity in stool collected on day 3. These findings are in agreement with previous studies, which showed that a high degree of temporal variation exists between faecal and urine samples.[27, 48] It should also be emphasised that host urinary metabolic composition is a manifestation of the interplay between the host homeostasis and gut microbial interactions with the environment. Hence, urinary metabolic composition is more regulated by the host as compared to faecal microbe composition which interacts directly with the diet and environment. Our results also indicate the need for extra caution when correlating host-gut microbiome systemic data as the delay in manifestation of urinary metabolic effect from the gut microbiota could lead to misinterpretation of the link between host metabolism and the functional role of gut microbiota.

Separation of the urine metabolite profiles collected on day 8 from other time points was mainly due to the relative increase in microbial-mammalian co-metabolites such as trimethylamine, trimethylamine N-oxide and phenylacetylglycine, and concomitant decrease in tricarboxylic acid cycle intermediates such as 2-oxoglutarate, citrate and pyruvate (Supplementary Table S1). However, the opposite was observed in level of hippurate, a known microbial-mammalian co-metabolite.[11, 49, 50] Hippurate is formed by glycine conjugation of benzoate in the liver, which is produced from bacterial metabolism of plant phenols[51] or quinic acid.[52] In addition, the gut microbiota is also involved in the catabolism of aromatic amino acids including tyrosin and tryptophan.[53] Significant changes in urinary microbial-mammalian co-metabolites observed on day 8 in the current work indicated a change in bacterial metabolism of phenolics in the animals. A variation in the composition of bacteria in the host could also explain the directionality of change in certain microbial-mammalian co-metabolites such as hippurate and phenyacetylglycine. The evidence of systemic gut microbe modulations was also found in the cross modelling analyses (Table 3). A series of host bacteria co-metabolites accounted for the highest explanatory values to gut microbe compositional change such as

dimethylamine (2.77 ppm), fumarate (6.55 ppm), hippurate (3.99 ppm), and α-hydroxy *N*-valerate (0.93 ppm). The same was observed with the re-labelled table after accounting for temporal delay between the two biological compartments with 2,3-dihydroxybutyrate (1.223 ppm) explaining 50% of the total R^2 value (~ 27%).

Further indicators of gut microbe perturbation were observed with changes in metabolites of choline metabolism, the methylamines, such as trimethylamine, trimethylamine *N*-oxide and dimethylglycine.[54, 55] Choline metabolism involves both mammalian and sym-xenobiotic metabolic pathways that are regulated through complex host-symbiont interaction.[56] Methylamines are also known to be co-metabolised by the host and the gut microbiota in the large intestine.[54] Changes in choline metabolites were only observed from day 8 onwards possibly indicating that perturbation in gut microbes involved in choline metabolism occur on day 8. In addition, significant increases in the level of urinary SCFAs such as 3-D-hydroxybutyrate and α-hydroxy *N*-valerate were also observed from day 8 onwards. SCFAs and lactic acid were products of bacterial fermentation of carbohydrates in the cecum and colon.[57, 58] Our observations are consistent with a previous animal study by Li *et al*.[27], which showed increases in SCFAs during later time points of acclimatisation.

Conclusion

Animal handlings such as lifting, cage changing and biological sample collections are common in animal studies. In this work, we showed that routine laboratory procedures during acclimatisation may affect the stress levels of mice resulting in modifications to the metabolic and gut microbiota composition. We would like to suggest that stress biomarkers such as corticosteroid levels be monitored when conducting an animal study in order to track animal stress levels throughout the study.[32] Additionally, animal handling intervals should be consistent especially in the murine model to minimise variations in stress levels, which could further complicate the extraction and interpretation of biological information.

Acknowledgement

We thank the editor and two anonymous reviewers for the helpful comments in improvement of the manuscript. We are grateful to International Medical University for the support and facilities of this work. This research is supported by Ministry of Science, Technology and Innovation eScience grant (02-02-09-SF0033). NMR signal processing and multivariate in-house software was developed by Dr. O. Cloarec, Dr. T. Ebbels, Dr. Kirill A. Veselkov, Dr. H. Keun and Dr. M. Rantalainen (Biomolecular Medicine, Department of Surgery and Cancer, Imperial College London). The authors also gratefully acknowledge the NMR facilities and assistance provided by Atta-ur-Rahman Institute for Natural Products Discovery, Universiti Teknologi MARA (UiTM), Puncak Alam Campus, Selangor, Malaysia.

References

1. N. Rosenthal and S. Brown, *Nat Cell Biol*, 2007, **9**, 993-999.
2. S. H. Yang, P. H. Cheng, H. Banta, K. Piotrowska-Nitsche, J. J. Yang, E. C. Cheng, B. Snyder, K. Larkin, J. Liu, J. Orkin, Z. H. Fang, Y. Smith, J. Bachevalier, S. M. Zola, S. H. Li, X. J. Li and A. W. Chan, *Nature*, 2008, **453**, 921-924.
3. A. L. Goodman, G. Kallstrom, J. J. Faith, A. Reyes, A. Moore, G. Dantas and J. I. Gordon, *Proc Natl Acad Sci U S A*, 2011, **108**, 6252-6257.
4. J. Saric, J. V. Li, Y. Wang, J. Keiser, K. Veselkov, S. Dirnhofer, I. K. Yap, J. K. Nicholson, E. Holmes and J. Utzinger, *J Proteome Res*, 2009, **8**, 3899-3911.
5. M. E. Bollard, E. G. Stanley, J. C. Lindon, J. K. Nicholson and E. Holmes, *NMR Biomed*, 2005, **18**, 143-162.
6. C. Ansong, A. C. Schrimpe-Rutledge, H. D. Mitchell, S. Chauhan, M. B. Jones, Y. M. Kim, K. McAteer, B. L. Deatherage Kaiser, J. L. Dubois, H. M. Brewer, B. C. Frank, J. E. McDermott, T. O. Metz, S. N. Peterson, R. D. Smith, V. L. Motin and J. N. Adkins, *Mol Biosyst*, 2013, **9**, 44-54.
7. B. L. Deatherage Kaiser, J. Li, J. A. Sanford, Y. M. Kim, S. R. Kronewitter, M. B. Jones, C. T. Peterson, S. N. Peterson, B. C. Frank, S. O. Purvine, J. N. Brown, T. O. Metz, R. D. Smith, F. Heffron and J. N. Adkins, *PLoS One*, 2013, **8**, e67155.
8. S. Madhavan, Y. Gusev, T. G. Natarajan, L. Song, K. Bhuvaneshwar, R. Gauba, A. Pandey, B. R. Haddad, D. Goerlitz, A. K. Cheema, H. Juhl, B. Kallakury, J. L. Marshall, S. W. Byers and L. M. Weiner, *Front Genet*, 2013, **4**, 236.
9. A. E. Perez-Cobas, M. J. Gosalbes, A. Friedrichs, H. Knecht, A. Artacho, K. Eismann, W. Otto, D. Rojo, R. Bargiela, M. von Bergen, S. C. Neulinger, C. Daumer, F. A. Heinsen, A. Latorre, C. Barbas, J. Seifert, V. M. dos Santos, S. J. Ott, M. Ferrer and A. Moya, *Gut*, 2013, **62**, 1591-1601.
10. J. V. Li, H. Ashrafian, M. Bueter, J. Kinross, C. Sands, C. W. le Roux, S. R. Bloom, A. Darzi, T. Athanasiou, J. R. Marchesi, J. K. Nicholson and E. Holmes, *Gut*, 2011, **60**, 1214-1223.
11. I. K. Yap, J. V. Li, J. Saric, F. P. Martin, H. Davies, Y. Wang, I. D. Wilson, J. K. Nicholson, J. Utzinger, J. R. Marchesi and E. Holmes, *J Proteome Res*, 2008, **7**, 3718-3728.
12. P. J. Turnbaugh and J. I. Gordon, *Cell*, 2008, **134**, 708-713.
13. F. P. Martin, M. E. Dumas, Y. Wang, C. Legido-Quigley, I. K. Yap, H. Tang, S. Zirah, G. M. Murphy, O. Cloarec, J. C. Lindon, N. Sprenger, L. B. Fay, S. Kochhar, P. van Bladeren, E. Holmes and J. K. Nicholson, *Mol Syst Biol*, 2007, **3**, 112.
14. F. P. Martin, N. Sprenger, I. K. Yap, Y. Wang, R. Bibiloni, F. Rochat, S. Rezzi, C. Cherbut, S. Kochhar, J. C. Lindon, E. Holmes and J. K. Nicholson, *J Proteome Res*, 2009, **8**, 2090-2105.
15. J. Han, L. C. Antunes, B. B. Finlay and C. H. Borchers, *Future Microbiol*, 2010, **5**, 153-161.
16. J. G. Fox, Y. Feng, E. J. Theve, A. R. Raczynski, J. L. A. Fiala, A. L. Doernte, M. Williams, J. L. McFaline, J. M. Essigmann, D. B. Schauer, S. R. Tannenbaum, P. C. Dedon, S. A. Weinman, S. M. Lemon, R. C. Fry and A. B. Rogers, *Gut*, 2010, **59**, 88-97.
17. S. P. Claus, S. L. Ellero, B. Berger, L. Krause, A. Bruttin, J. Molina, A. Paris, E. J. Want, I. de Waziers, O. Cloarec, S. E. Richards, Y. Wang, M. E. Dumas, A. Ross, S. Rezzi, S. Kochhar, P. Van Bladeren, J. C. Lindon, E. Holmes and J. K. Nicholson, *MBio*, 2011, **2**, e00271-00210.
18. M. E. Bollard, E. Holmes, J. C. Lindon, S. C. Mitchell, D. Branstetter, W. Zhang and J. K. Nicholson, *Anal Biochem*, 2001, **295**, 194-202.
19. M. C. Noverr and G. B. Huffnagle, *Trends in Microbiology*, 2004, **12**, 562-568.
20. C. L. Gavaghan, I. D. Wilson and J. K. Nicholson, *FEBS Lett*, 2002, **530**, 191-196.
21. E. G. Stanley, N. J. Bailey, M. E. Bollard, J. N. Haselden, C. J. Waterfield, E. Holmes and J. K. Nicholson, *Anal Biochem*, 2005, **343**, 195-202.
22. S. X. Wang and W. C. Wu, *World J Gastroenterol*, 2005, **11**, 2016-2021.
23. T. Poole, *Lab Anim*, 1997, **31**, 116-124.
24. J. P. Balcombe, N. D. Barnard and C. Sandusky, *Contemp Top Lab Anim Sci*, 2004, **43**, 42-51.
25. G. Jean Kant, T. Eggleston, L. Landman-Roberts, C. C. Kenion, G. C. Driver and J. L. Meyerhoff, *Pharmacology Biochemistry and Behavior*, 1985, **22**, 631-634.

26. K. Gouveia and J. L. Hurst, *PLoS One*, 2013, **8**, e66401.
27. J. V. Li, J. Saric, I. K. Yap, J. Utzinger and E. Holmes, *Mol Biosyst*, 2013, **9**, 3155-3165.
28. S. M. O'Mahony, J. R. Marchesi, P. Scully, C. Codling, A. M. Ceolho, E. M. Quigley, J. F. Cryan and T. G. Dinan, *Biol Psychiatry*, 2009, **65**, 263-267.
29. N. Sudo, Y. Chida, Y. Aiba, J. Sonoda, N. Oyama, X.-N. Yu, C. Kubo and Y. Koga, *The Journal of Physiology*, 2004, **558**, 263-275.
30. M. Matsumoto, R. Kibe, T. Ooga, Y. Aiba, S. Kurihara, E. Sawaki, Y. Koga and Y. Benno, *Sci. Rep.*, 2012, **2**.
31. E. Mostl and R. Palme, *Domest Anim Endocrinol*, 2002, **23**, 67-74.
32. C. Touma, R. Palme and N. Sachser, *Horm Behav*, 2004, **45**, 10-22.
33. O. Kalliokoski, J. Hau, K. R. Jacobsen, C. Schumacher-Petersen and K. S. Abelson, *Gen Comp Endocrinol*, 2010, **168**, 450-454.
34. C. W. Chong, D. A. Pearce, P. Convey and I. K. P. Tan, *Antarctic Science*, 2012, **24**, 249-258.
35. S. W. Culman, R. Bukowski, H. G. Gauch, H. Cadillo-Quiroz and D. H. Buckley, *BMC Bioinformatics*, 2009, **10**, 171.
36. C. J. Smith, B. S. Danilowicz, A. K. Clear, F. J. Costello, B. Wilson and W. G. Meijer, *FEMS Microbiol Ecol*, 2005, **54**, 375-380.
37. J. Trygg and S. Wold, *J Chemometr*, 2002, **16**, 119-128.
38. O. Cloarec, M. E. Dumas, J. Trygg, A. Craig, R. H. Barton, J. C. Lindon, J. K. Nicholson and E. Holmes, *Anal Chem*, 2005, **77**, 517-526.
39. R. A. S. Fisher, *The Design of Experiments*, Oliver & Boyd, Edinburgh ; London, 1935.
40. H. Yanagihara, K.-I. Kamo and T. Tonda, *Can J Stat*, 2011, **39**, 126-146.
41. M. P. Leussis and V. J. Bolivar, *Neurosci Biobehav Rev*, 2006, **30**, 1045-1064.
42. C. Kopp, F. Longordo, J. R. Nicholson and A. Luthi, *J Neurosci*, 2006, **26**, 12456-12465.
43. F. Longordo, J. Fan, T. Steimer, C. Kopp and A. Luthi, *Sleep*, 2011, **34**, 679-681.
44. G. W. Tannock and D. C. Savage, *Infect Immun*, 1974, **9**, 591-598.
45. M. Aguilera, P. Vergara and V. Martinez, *Neurogastroenterol Motil*, 2013, **25**, e515-529.
46. M. T. Bailey, S. E. Dowd, J. D. Galley, A. R. Hufnagle, R. G. Allen and M. Lyte, *Brain Behav Immun*, 2011, **25**, 397-407.
47. S. Zheng, M. Yu, X. Lu, T. Huo, L. Ge, J. Yang, C. Wu and F. Li, *Clin Chim Acta*, 2010, **411**, 204-209.
48. J. Saric, Y. Wang, J. Li, M. Coen, J. Utzinger, J. R. Marchesi, J. Keiser, K. Veselkov, J. C. Lindon, J. K. Nicholson and E. Holmes, *J Proteome Res*, 2008, **7**, 352-360.
49. B. L. Goodwin, C. R. Ruthven and M. Sandler, *Biochem Pharmacol*, 1994, **47**, 2294-2297.
50. H. J. Lees, J. R. Swann, I. D. Wilson, J. K. Nicholson and E. Holmes, *J Proteome Res*, 2013, **12**, 1527-1546.
51. A. J. Schwab, L. Tao, T. Yoshimura, A. Simard, F. Barker and K. S. Pang, *Am J Physiol Gastrointest Liver Physiol*, 2001, **280**, G1124-1136.
52. A. M. Asatoor, *Biochim Biophys Acta*, 1965, **100**, 290-292.
53. E. Diaz, A. Ferrandez, M. A. Prieto and J. L. Garcia, *Microbiol Mol Biol Rev*, 2001, **65**, 523-569, table of contents.
54. J. L. Smith, J. S. Wishnok and W. M. Deen, *Toxicol Appl Pharmacol*, 1994, **125**, 296-308.
55. S. H. Zeisel, K. A. DaCosta and J. G. Fox, *Biochem J*, 1985, **232**, 403-408.
56. M. E. Dumas, R. H. Barton, A. Toye, O. Cloarec, C. Blancher, A. Rothwell, J. Fearnside, R. Tatoud, V. Blanc, J. C. Lindon, S. C. Mitchell, E. Holmes, M. I. McCarthy, J. Scott, D. Gauguier and J. K. Nicholson, *Proc Natl Acad Sci U S A*, 2006, **103**, 12511-12516.
57. G. T. Macfarlane and S. Macfarlane, *Curr Opin Biotechnol*, 2007, **18**, 156-162.
58. D. L. Topping and P. M. Clifton, *Physiol Rev*, 2001, **81**, 1031-1064.
59. A. M. Neyrinck, V. F. Van Hee, L. B. Bindels, F. De Backer, P. D. Cani and N. M. Delzenne, *Br J Nutr*, 2013, **109**, 802-809.
60. N. P. McNulty, M. Wu, A. R. Erickson, C. Pan, B. K. Erickson, E. C. Martens, N. A. Pudlo, B. D. Muegge, B. Henrissat, R. L. Hettich and J. I. Gordon, *PLoS Biol*, 2013, **11**, e1001637.

61. A. Hakansson, N. Tormo-Badia, A. Baridi, J. Xu, G. Molin, M. L. Hagslatt, C. Karlsson, B. Jeppsson, C. M. Cilio and S. Ahrne, *Clin Exp Med*, 2014, **11**, 11.
62. J. M. Kinross, N. Alkhamesi, R. H. Barton, D. B. Silk, I. K. Yap, A. W. Darzi, E. Holmes and J. K. Nicholson, *J Proteome Res*, 2011, **10**, 277-287.
63. E. Skordi, I. K. Yap, S. P. Claus, F. P. Martin, O. Cloarec, J. Lindberg, I. Schuppe-Koistinen, E. Holmes and J. K. Nicholson, *J Proteome Res*, 2007, **6**, 4572-4581.

Figure Captions

Fig 1. (A) PCA scores plot (R^2, 32.1%) derived from faecal TRFLP of female BALB/c mice from day 1 (green), day 2 (blue), day 3 (red), day 8 (orange) and day 15 (turqouise). (B) Corresponding PCA mean trajectory plot derived from the same TRFLP profiles as (A). Error bar indicates standard error. Key: D1, day 1; D2, day 2; D3, day 3; D8, day 8; D15, day 15

Fig 2. (A) PCA scores plot (R^2, 36.1%) derived from ^{1}H NMR urinary spectra of female BALB/c mice from day 1 (green), day 2 (blue), day 3 (red), day 7 (orange) and day 14 (turqouise). (B) Corresponding PCA mean trajectory plot derived from the same ^{1}H NMR urinary spectra as (A). Error bar indicates standard error. Covariance plot showing the colour-coded significance of urinary metabolite profiles calculated using permutation test between (C) day 1 and day 8, and (D) day 8 and day 15. Key: D1, day 1; D2, day 2; D3, day 3; D8, day 8; D15, day 15

Figures

Figure 1

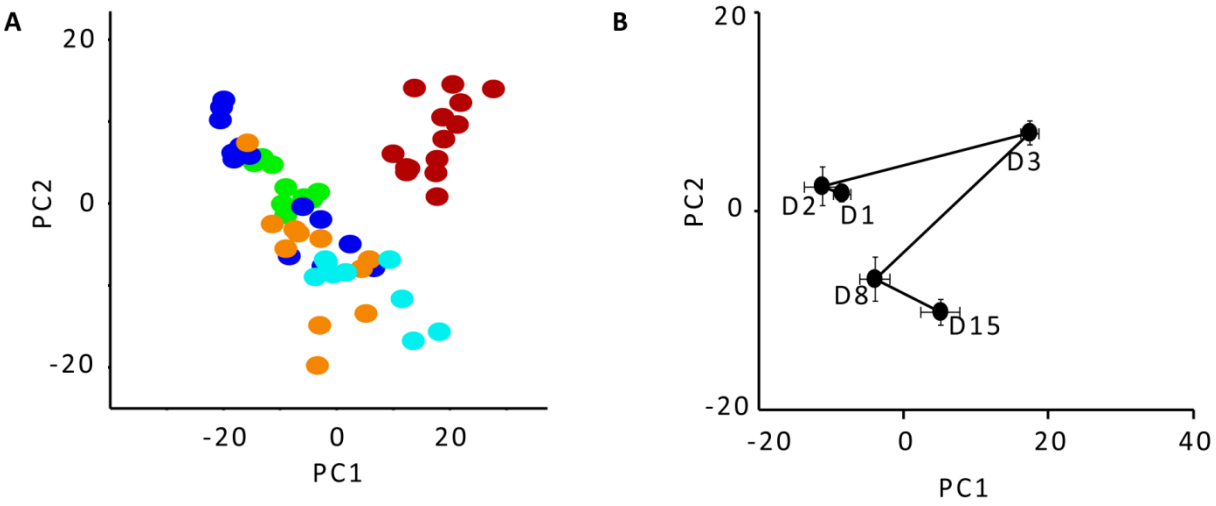

Figure 2

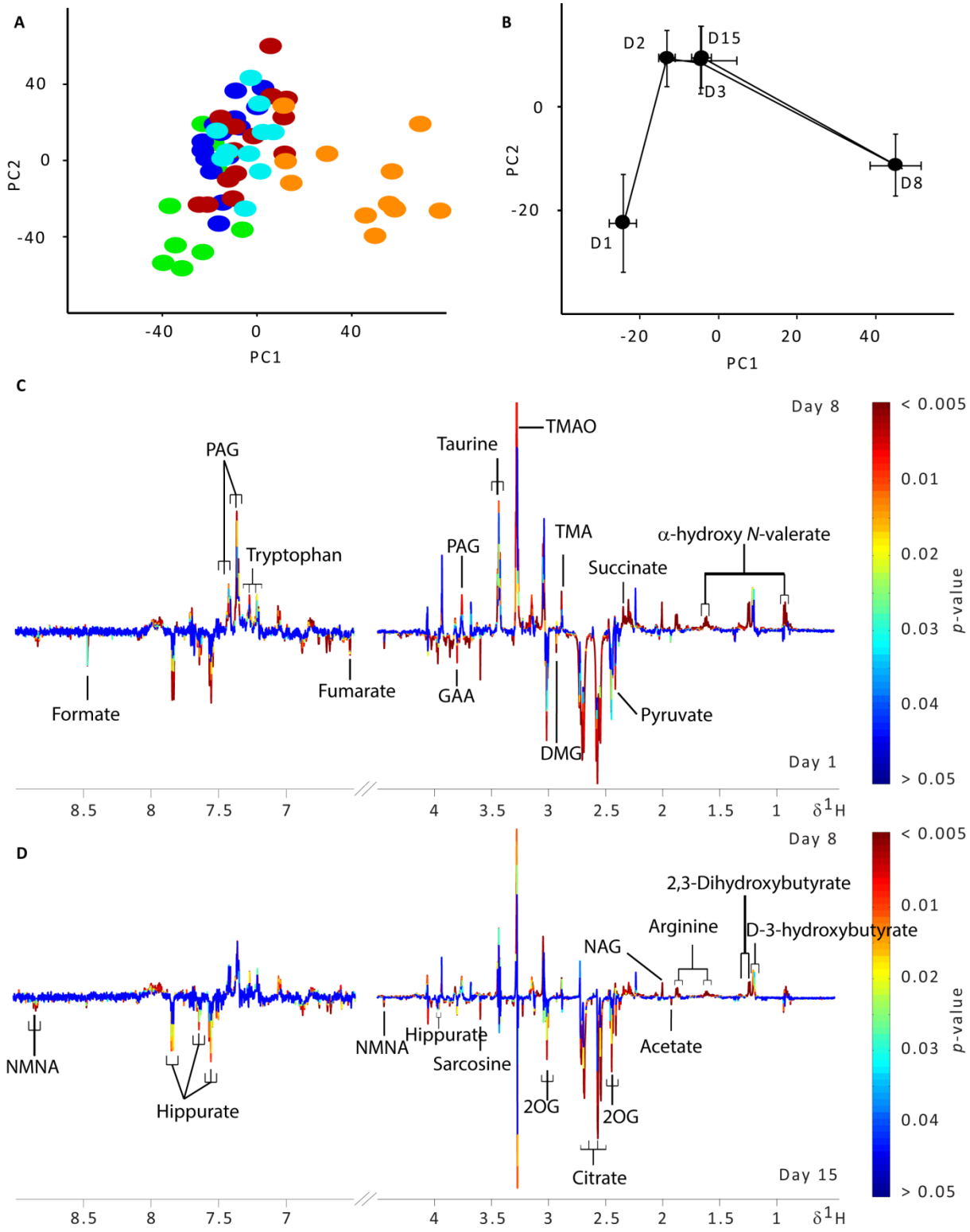

Tables

Table 1. Period of acclimatisation reported in selected metagenomics or/and metabonomics studies.

Study	Period of acclimatisation	Type of animals	References
Dietary effects on tissue inflammation, hypercholesterolaemia and gut microbiota	1 week	Male Balb/c mice	[59]
Ability of gut microbes to adapt to dietary perturbations	Not stated	Male germ-free C57BL/6J mice	[60]
Immunological alteration and changes of gut microbiota to dextran sulfate sodium administration	Not stated	Wild-type female C57BL/6 mice	[61]
Metabolic profiling on batch and age-related changes	Not stated	Female NMRI mice	[27]
Metabolic phenotyping in experimental laparotomy model of surgical trauma	1 week	Male Wistar rats	[62]
Metabonomics and microbiological studies of vancomycin-induced changes	1 week	Female NMRI mice	[11]
Metabonomics study of ethionine-induced metabolic changes	10 days	Male HanWistar rats	[63]

Table 2. Corticosterone levels and bacterial diversity (mean±SE) in the faecal samples. Different letters in superscript denote significant difference at $P < 0.05$.

Days	Corticosterone level (log pg/mL)	Total TRFLP peaks	Shannon diversity index (*H'*)	Diversity evenness (*J'*)
1	6.87^{A} ±0.12	309.3^{B} ±13.1	4.69^{CD} ±0.09	0.82^{CD} ±0.013
2	6.80^{AB} ±0.09	178.1^{C} ±33.3	4.30^{D} ±0.19	0.87^{D} ±0.010
3	6.53^{B} ±0.05	530.9^{A} ±14.3	5.73^{A} ±0.03	0.91^{A} ±0.005
8	6.70^{AB} ±0.03	283.4^{B} ±25.0	4.95^{BC} ±0.17	0.88^{BC} ±0.017
15	6.75^{AB} ±0.05	337.4^{B} ±13.1	5.34^{AB} ±0.08	0.92^{AB} ±0.014

Table 3. Cross modelling of urine metabolite and T-RFLP profiles using stepwise selection procedure. Note: Prop. = explanatory proportion, Cumul. = cumulative explanatory proportion, res.df = residual degree of freedom. [a] +, inclusion; - exclusion.

A. Modelling of urine metabolite pattern using gut microbial composition as predictors

Variable[a]	AICc	SS(trace)	Pseudo-F	P	Prop.	Cumul.	res.df
+59G	315.35	1189.1	5.3738	0.001	8.76E-02	8.76E-02	56
+252G	314.55	630.09	2.9464	0.003	4.64E-02	0.13395	55
+350B	313.72	619.2	3.0008	0.005	4.56E-02	0.17955	54
+217B	312.64	649.46	3.2804	0.002	4.78E-02	0.22737	53
+310G	311.61	618.03	3.2544	0.002	4.55E-02	0.27287	52
+61B	310.91	544.78	2.9778	0.006	4.01E-02	0.31299	51
+372B	310.66	462.65	2.6086	0.017	3.41E-02	0.34705	50
+431G	310.55	435.7	2.5319	0.071	3.21E-02	0.37913	49
+424B	310.42	434.17	2.6057	0.047	3.20E-02	0.4111	48

B. Modelling of gut microbial composition using urine metabolite profile as predictors

Variable[a]	AICc	SS(trace)	Pseudo-F	P	Prop.	Cumul.	res.df
+3.982	383.58	2851	3.9732	0.001	6.62E-02	6.62E-02	56
+2.765	381.88	2630.6	3.8527	0.001	6.11E-02	0.12738	55
+6.546	381.5	1704.6	2.5677	0.001	3.96E-02	0.16699	54
+3.142	381.16	1651.7	2.5598	0.013	3.84E-02	0.20536	53
+3.991	380.93	1571.1	2.504	0.002	3.65E-02	0.24187	52
-3.982	380.15	977.69	1.5583	0.027	2.27E-02	0.21915	53
+0.934	379.75	1631.3	2.6532	0.001	3.79E-02	0.25706	52
+6.993	379.63	1464.3	2.4479	0.001	3.40E-02	0.29109	51